CONSTRAINTS ON CRATER AGES ON RHEA FROM CASSINI VIMS AND ISS: INSIGHTS TO THE RECENT CRATER FLUX. E. G. Rivera-Valentín[1], M. R. Kirchoff[2], C. M. Dalle Ore[3], C. Rodriguez Sanchez-Vahamonde[4]; [1]Lunar and Planetary Institute & Arecibo Observatory, Universities Space Research Association, Houston, TX (ervalentin@usra.edu), [2]Southwest Research Institute, Boulder, CO, [3]SETI Institute, Mountain View, CA, [4]Arecibo Observatory, Universities Space Research Association, Arecibo, PR.

Introduction: The Saturnian satellites are dominated by H_2O ice as deduced from the characteristic spectral signature in the near-infrared (1-5 μm). The 1.65-μm H_2O ice band, seen in both ground based spectra and in data from the Cassini Visible and Infrared Mapping Spectrometer (VIMS), indicates the presence of the hexagonal crystalline form. During a hypervelocity impact onto such an icy moon, a shallow quasi-spherical melt region is produced [1,2]. Crystalline ice forms from the flash heating and cooling of the exposed melt [3]. Over time, bombardment by ions disrupts the crystalline structure producing amorphous ice [4,5]. The surface temperature of Saturn's mid-sized moons is in the range where the amorphous phase is stable over the age of the Solar System [6]. Therefore, the local abundance of amorphous ice with respect to crystalline ice within and surrounding craters allows for an estimate of crater formation age [7].

Such a technique is invaluable, especially considering that the cratering flux for the outer Solar System is severely lacking constraints, unlike the inner Solar System, which has geochronological measurements of returned lunar samples and martian meteorites combined with cratering studies. Ages of large craters paired with crater statistical analysis of the crater's interior floor can then inform on the recent outer Solar System crater flux. Here we discuss preliminary results of the project by studying craters on Rhea, specifically Obatala, Inktomi, and Wakonda.

Ice Phase Distribution: H_2O ice phase can be determined based on a few key differences in the spectral signature. The most obvious and commonly adopted is the depth of the 1.65-μm band. In the case of our data, we are precluded from using this band as it corresponds to one of the VIMS instrument's filter junction. Furthermore, the band is highly biased by the presence of even traces of crystalline H_2O ice [8] and cannot yield a precise measure of the fraction of one phase versus the other. We therefore adopt the 2.0-μm band whose shape is affected by changes in phase [9] in a consistent way. By measuring the distortion on models with varying amounts of crystalline to amorphous H_2O ice we calibrate the effects of phase change in the spectra. We then apply the calibration to measurements of distortion performed on the data and obtain a crystallinity fraction. From the relative amount of crystalline to amorphous H_2O ice and information about the flux of infalling energetic particles on the area, we can estimate the age of the craters making use of the equation given in [3].

So far only Obatala has yielded an age, previously reported in [7] of ~450 Ma. The location of Inktomi (leading hemisphere), though, has largely shielded it from charged particle bombardment considered responsible for phase transition. Because Rhea's orbital speed is slower than the rate at which the Saturnian magnetosphere revolves around the planet, charged particles preferentially impact Rhea's trailing hemisphere [10]. However, the shape, distribution, and relative amounts of crystalline to amorphous H_2O ice make Inktomi the younger of the two craters. Indeed, Inktomi has roughly 20% more crystalline ice than Obatala [7]. We are presently working on the ice phase distribution of Wakonda and other craters. Updates will be presented at the meeting.

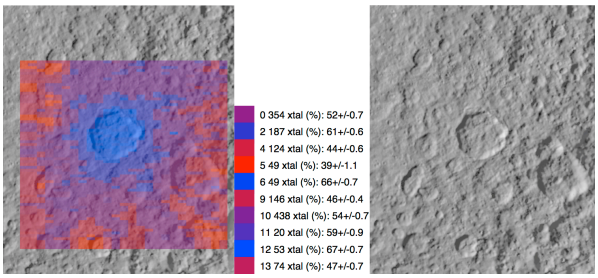

Fig. 1: Map of varying water ice phase across the Inktomi crater region on Rhea overlain on an ISS image (PIA14928 composite from Cassini and Voyager images by SSI/CICLOPS imaging team), also shown on the right for ease of comparison. The legend lists the class number and corresponding population followed by the percentage of crystalline ice and its uncertainty.

Cratering History: To get new constraints on the recent cratering flux, we examine the distributions of smaller craters formed on the floors of the larger craters examined in the ice phase distribution task. The initial step is to find the highest resolution Cassini ISS image(s) with solar incidence angles between 50º-80º of the larger craters and integrate them into JMARS. We select the highest resolution images to get constraints on the flux of the smallest craters possible, and the solar incidence angle range is required to robustly identify all small craters.

Once images are integrated, we use JMARS' 3-point crater measurement tool to measure the small, superposed crater diameters and positions. This information is then used to generate crater size-frequency distributions (SFDs) in both the cumulative and relative (R-plot) formats [11; Fig. 2]. We use a new, more statistically robust technique to compute the crater SFDs that uses a kernel density estimator and bootstrap calculation of the uncertainties [12]. These incorporate a more accurate representation of the uncertainties involved in both identifying and measuring craters.

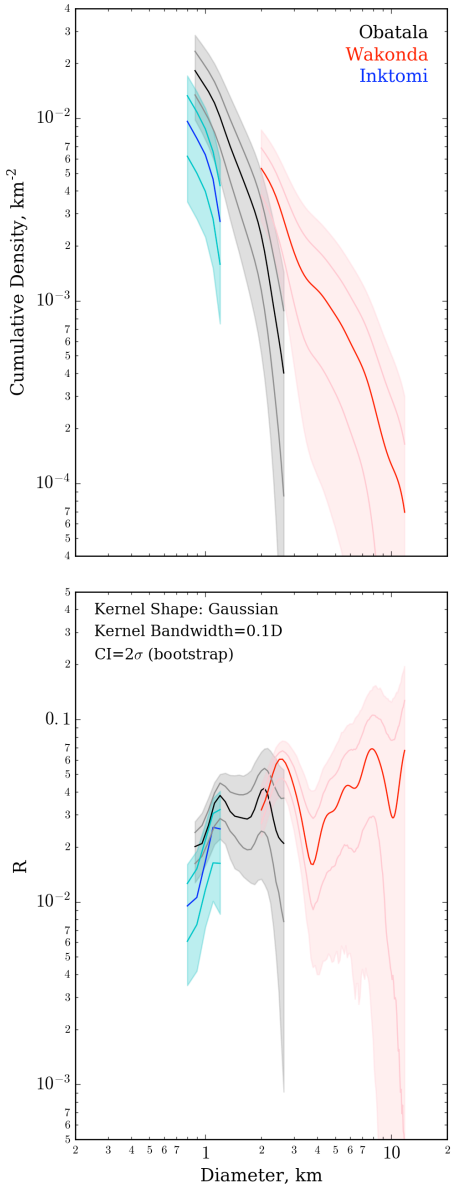

Fig. 1: Cumulative (top) and relative (bottom) superposed crater SFDs on the floors of Obatala, Wakonda, and Inktomi. Solid, thick lines designate the crater SFDs. Solid, thin lines designate the 1σ bootstrap confidence interval (CI), while shaded areas designate the 2-σ bootstrap CI.

Figure 2 shows the superposed crater SFDs for Obatala, Wakonda and Inktomi on Rhea. Comparison indicates Wakonda has a slightly higher superposed crater density, $N(2)=5.31(+3.31/-2.58)\times10^{-3}$ km^{-2}, than Obatala, $N(2)=2.28(+2.77/-1.77)\times10^{-3}$ km^{-2}; however, the difference is not large (t_{value}=0.78) suggesting that variations in ice phase distribution between these craters may not be significant. Crater densities between Obatala, $N(1)=1.40(+0.85/-0.7)\times10^{-2}$ km^{-2}, and Inktomi, $N(1)=0.63(+0.50/-0.41)\times10^{-2}$ km^{-2}, show that the latter has a lower superposed crater density, though, again the difference is not significant (t_{value}=0.89) after accounting for 2-σ error. Furthermore, the similarity of the shape of the crater SFDs also indicates the shape of the impactor SFD has not significantly changed between the formation of the studied craters.

Conclusions: Here we use a novel method, inferred crater formation age through ice phase distribution [7], paired with crater density studies to constrain the early crater flux of the Saturnian system.

Our results of ice phase relative ages (derived by relative abundance of amorphous ice to crystalline ice) are supported by the measured crater densities, providing confidence in the technique. The studied craters may have formed in the following sequence: Wakonda, Obatala, and Inktomi. The cumulative crater density difference between the formation of Wakonda and Obatala is $\Delta N(2)=3.03(+5.08/-5.35)\times10^{-3}$ km^{-2}, while for Obatala and Inktomi is $\Delta N(1)=0.77(+1.26/-1.20)\times10^{-2}$ km^{-2}. A zero solution for ΔN between each studied crater cannot be ruled out because the crater densities at 2-σ intersect, suggesting that they potentially formed concurrently. However, for the case of Obatala and Intkomi, at least, the relative ice phase age suggests Obatala is older. Results for Wakonda will be discussed at the conference. Furthermore, we find the impactor SFD did not significantly change during the formation of these craters, suggesting a nearly constant source population, for at least the last 450 Ma.

References: [1] Pierazzo, E., et al. (1997) *Icarus*, 127, 408-423. [2] Barr, A. C. and Citron, R. I. (2011) *Icarus*, 211, 913-916. [3] Baragiola, R. A., et al. (2013) *The Science of Solar System Ices*, 356, 527-549. [4] Mastrapa, R. M. and Brown, R. H. (2006) *Icarus*, 183, 207-214. [5] Baragiola, R. A. (2003) *Planetary and Space Science*, 51, 953-961. [6] Mastrapa, R. M., et al. (2013) *The Science of Solar System Ices*, 356, 371-408. [7] Dalle Ore, C. M., et al. (2015) *Icarus*, 261, 80-90. [8] Mastrapa, R. M., et al. (2008) *Icarus*, 197, 307-320. [9] Grundy, W. M. and Schmitt, B. (1998) *JGR*, 103, 25809-25822. [10] Schenk, P. M., et al. (2011) *Icarus*, 211, 740-757. [11] Crater Analysis Techniques Working Group (1979) *Icarus*, 37, 467-474. [12] Robbins, S. et al. (2018) *MAPS*, in press.

Acknowledgements: This material is based upon work supported by NASA through the Cassini Data Analysis Program under Grant No. NNX17AG01G.